Characteristics of inertia-gravity waves revealed in rawinsondes at Jang Bogo Station (JBS), Antarctica (74.374°S, 164.137°E)

Ji-hee Yoo[1], Tae-Jin Choi[2] , Hye-Yeong Chun[1], Young-Ha Kim[3], In-Sun Song[2], and Byeong-Gwon Song[1]

[1] *Department of Atmospheric Sciences, Yonsei University, Seoul, Republic of Korea*
[2] *Division of Polar Climate Research, Korea Polar Research Institute, Republic of Korea*
[3] *Institut für Atmosphäre und Umwelt, Goethe Universität Frankfurt, Germany*

Introduction

- The importance of **atmospheric gravity waves (GWs)** in determining middle atmosphere circulation has been examined by various observational studies.
- In particular, **radiosonde observations** provide direct measurements of wind and temperature covering over an extensive geographical and temporal range [Ki and Chun, 2010].
- In this study, high vertical resolution rawinsonde data collected at **Jang Bogo Station (JBS)**, Antarctica (74˚374'S and 164˚137'E) from 2014 to 2016 are analyzed. JBS is the **second Korean Antarctic research station**, constructed in 2014 in Terra Nova Bay, Antarctica.
- Using the rawinsonde observations, we examine

(1) wind and temperature structure observed from rawinsonde at JBS, and **make comparisons** with four reanalysis data **(CFSv2, MERRA, ERA-Interim, and NCEP/DOE R2)**

(2) characteristics of inertia-gravity waves (IGWs) in the troposphere and the lower stratosphere using **stokes parameter** method based on **quasi-monochromatic wave** theory.

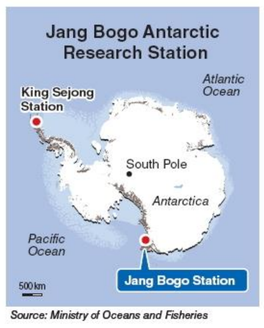

Figure 1. Geographical location of Jang Bogo Station at Terra Nova Bay

Data

Rawinsonde data		
Model		Vaisala GPS sonde RS92G
Variables		zonal wind (U), meridional wind (V), temperature (T), and pressure (P)
Period		December 2014–December 2016 (25 months)
Launch frequency		Once a day (at 00 UTC)
Resolution	Temporal	2 second
	Vertical	~10 m

Reanalysis data					
Data set		CFSv2	MERRA	ERA-Interim	NCEP/DOE R2
Variables		zonal wind (U), meridional wind (V), temperature (T), pressure (P)			
Period		December 2014–December 2016 (24 months)			
Resolution	Temporal	1 day (at 00 UTC)			
	Horizontal	2.5˚ × 2.5˚	1.5˚ × 1.5˚	0.5˚ × 0.5˚	1.25˚ × 1.25˚
	Vertical (Model Top)	17 levels (10 hPa)	37 levels (1 hPa)	37 levels (1 hPa)	42 levels (0.1 hPa)

Wind and Temperature structures at JBS

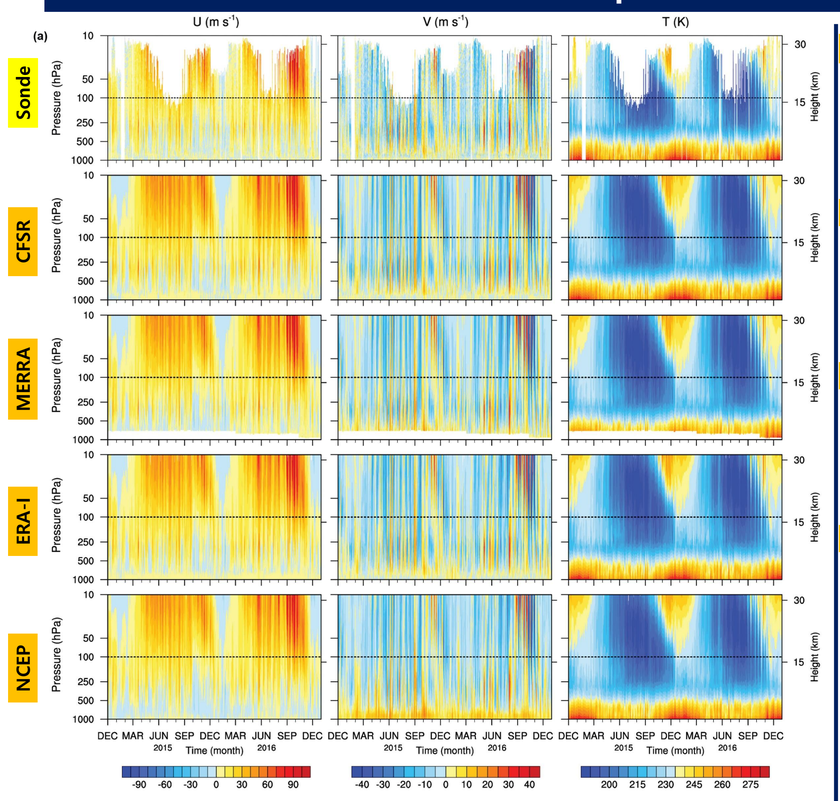

Figure 2. Time-height cross sections of the zonal wind (U) (first column), meridional wind (V) (second column), and temperature (T) (third column) revealed in the rawinsonde observations and the four reanalysis datasets: CFSv2, MERRA, ERA-Interim, and NCEP/DOE R2. Dotted line represents 100 hPa for an easier comparison.

- In the stratosphere, **westerlies** are dominant from **Mar. to Nov.** with **the maximum speed of 122 m s^{-1}** in 2016, while **weak westerlies** and **easterlies** appear alternately in the troposphere**.**
- The lowest temperature of 179 K appears at about 20 km in **Sep.**
- Spring warming occurs from the upper stratosphere in **Sep.** and propagates downward to the lower stratosphere until **Nov.**

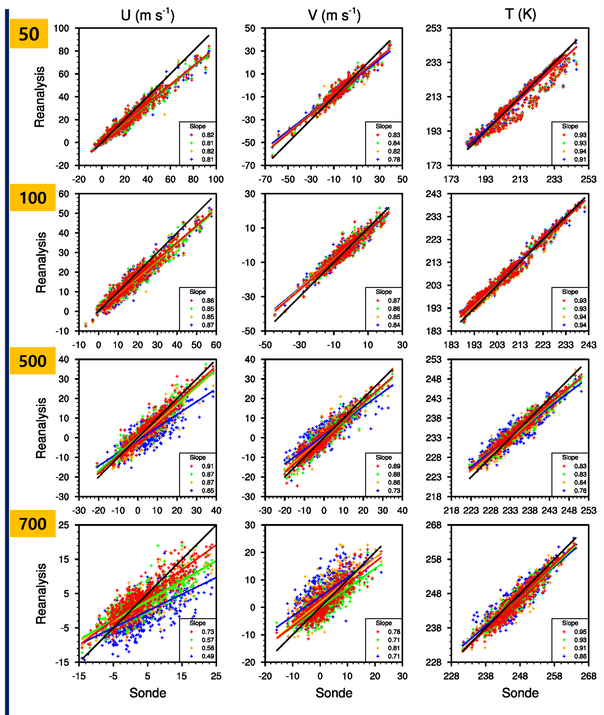

Figure 3. Scatterplot of zonal (first column) wind, meridional (second column) wind, and temperature (third column) from four reanalysis datasets at 50 hPa, 100 hPa, 500 hPa, and 700 hPa. The red, blue, cyan, and orange lines represent the CFSv2, MERRA, ERA-Interim, and NCEP/DOE R2 datasets, respectively.

- At **700 hPa**, reanalysis data with coarse resolution **(NCEP R2 and MERRA)** have strong **negative (positive)** bias in **zonal (meridional)** wind.
- **Precision** and **accuracy** increase with height.
- **Underestimation of the polar vortex** and **too cold stratosphere** in all four reanalysis datasets

Investigation of inertia-gravity waves (IGWs) revealed in rawinsonde data

Wave analysis method

- To avoid the effect of the **tropopause**, wave analysis is conducted in the **troposphere (2-7 km)** and **stratosphere (15-22 km)** [Ki and Chun, 2010]**.**
- Extraction of GWs **[Vincent et al., 1997]**
  - ✓ **Basic state** $\bar{\psi}$: 3rd order polynomial using the least-square method
  - ✓ **GW components:** U,V, and T perturbation $\psi' = \psi - \bar{\psi}$

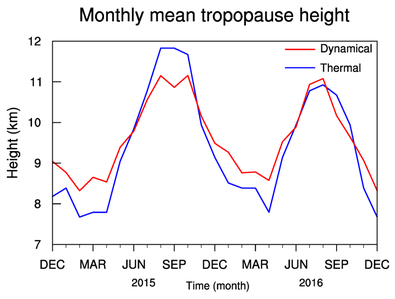

Figure 4. Tropopause height above JBS from December 2014 to December 2016, which is calculated using model-level ERA-Interim.

➢ Conditions for **IGW** : 1) *degree of polarization* $(\boldsymbol{dp}) > \mathbf{0.5}$
2) $\boldsymbol{f < \hat{\omega} \leq 10f}$

	Troposphere	Stratosphere
the number of satisfying IGW/ the number of available profiles	334 / 727 (46 %)	397 / 554 (70 %)

Wave vertical propagation direction

$$R = \frac{ACW}{ACW+CW} > 0.5: \text{ upward E propagation}$$

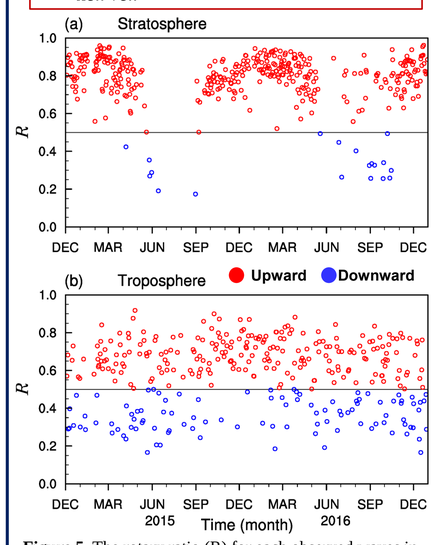

Figure 5. The rotary ratio (R) for each observed waves in the stratosphere (upper) and troposphere (lower).

- **In the stratosphere**, **down-going IGWs** appear only from **Apr. to Oct.** (Murphy et al., 2014; Sato and Yoshiki, 2008)
  - ▶ Possibly generated from **polar-night jet**
- **In the troposphere, the seasonal variations** of down-going IGWs **are not obvious.**
  - **1) GW source lying intermediate layer between two layers**
  - **2) Reflection of up-going IGWs**

Wave horizontal propagation direction

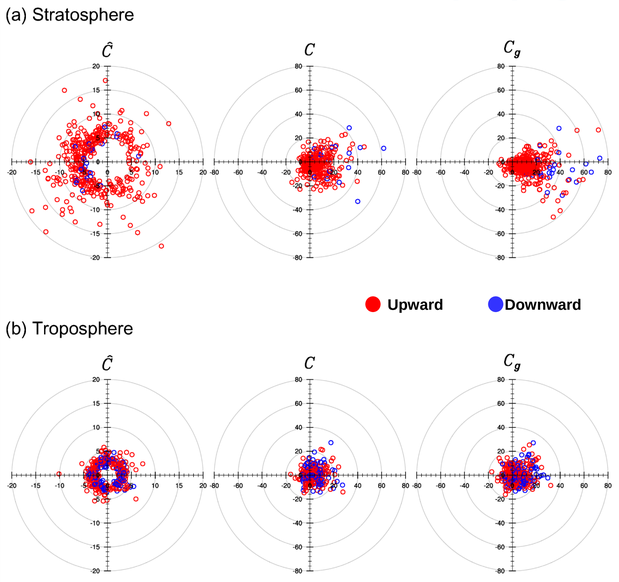

Figure 6. Intrinsic phase velocity $\hat{C}$ (first column), phase velocity C (second column) and ground-based group velocity C_g(third column) in the stratosphere (upper) and troposphere (lower).

- **In the troposphere**, $\hat{C}$ are nearly **isotropic, while** many of the IGWs **in the stratosphere** have **westward** $\hat{C}$.
- Given that most of the phase speeds are **eastward**, up-going **IGWs with C less than the background westerlies** tend to be observed in the stratosphere without **critical level filtering**.
- Due to the prevailing **westerly in the stratosphere**, IGWs are advected to eastward (positive C_g).

Wave energy

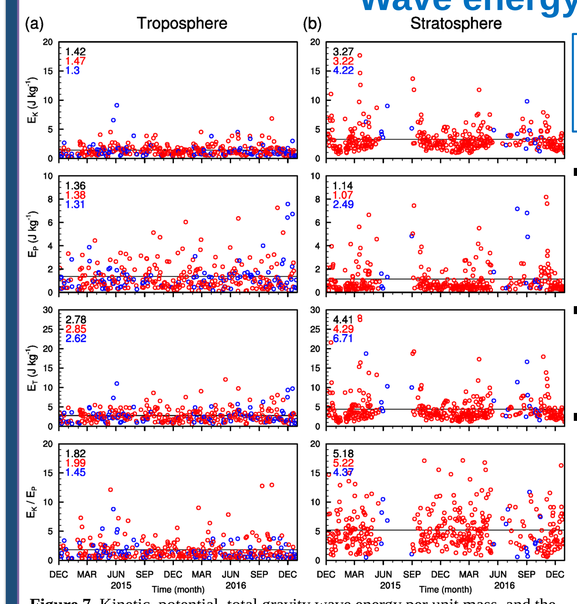

$$E_T = E_k + E_p = \frac{1}{2}\left[\overline{u'^2} + \overline{v'^2} + \overline{w'^2}\right] + \frac{1}{2}\left[\frac{g^2}{N^2}\left(\overline{\frac{T'}{\bar{T}}}\right)^2\right]$$

- Stronger GW activity in the stratosphere $(\boldsymbol{E_T = 4.41J\ kg^{-1}})$ than in the troposphere $(\boldsymbol{E_T = 2.78J\ kg^{-1}})$**.**
- **Obvious seasonal variations in E_K** and **E_P** in the Stratosphere
- Mean ratio **E_K / E_P ~ 5.18 (1.82) in the stratosphere (troposphere)** is much higher than the theoretical value **(3/5 <the ratio <2)**.
  - ▶ **Momentum sources** for GWs is suggested.

Figure 7. Kinetic, potential, total gravity wave energy per unit mass, and the ratio of kinetic to potential energy in the troposphere and the stratosphere. The number at the upper left corner is the average values for up-going (red) and down-going waves

Intrinsic frequency and Wavelengths

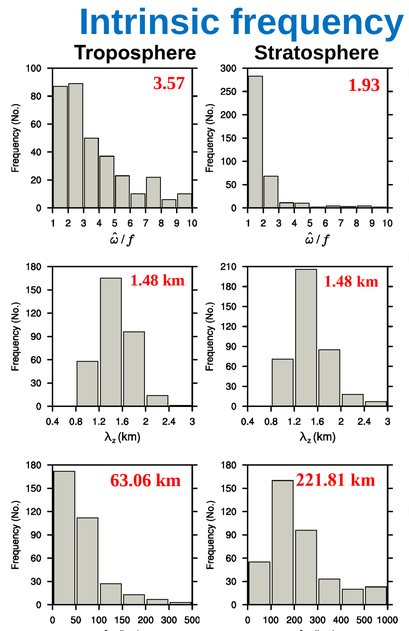

Figure 8. Histogram of $\hat{\omega}$ / f (upper), λ_z(middle), and λ_h(lower) calculated in the troposphere (left) and stratosphere (right).

- **Higher intrinsic frequency $(\hat{\omega})$** in the troposphere (3.57) than in the stratosphere (1.81)
- Similar **vertical wavelengths (λ_z~1.48 km)** in both layers
- Due to smaller $\hat{\omega}/f$ and larger **N**, horizontal wavelength λ_h in the stratosphere (221 km) is much longer than that in the troposphere (63 km) by the dispersion relation

$$k_h^2 = \frac{m^2 f^2 [(\hat{\omega}/f)^2 - 1]}{N^2}$$

- Vertical and horizontal wavelengths are relatively shorter compared to those revealed in **the lower** and **mid-latitude regions.** [Murphy et al., 2014; Moffat-Griffin et al., 2011]

Gravity wave momentum flux

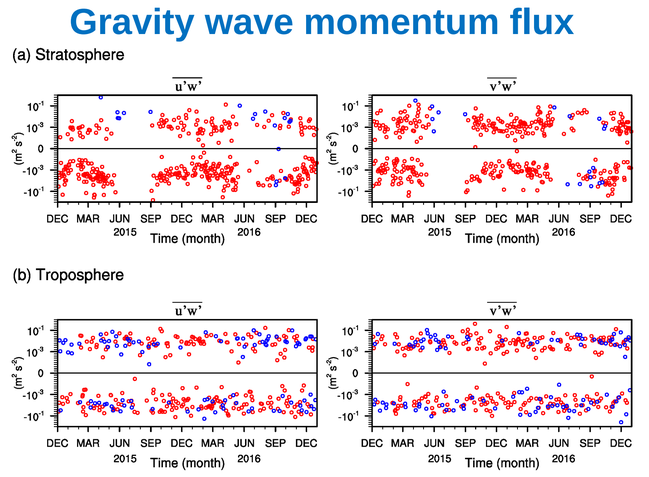

Figure 9. Vertically averaged momentum fluxes for upward (red) and downward (blue) propagating waves in the stratosphere (upper) and troposphere (lower).

$$\overline{u'w'} = \frac{g\hat{\omega}}{N^2}\overline{u'\left(\frac{T'}{\bar{T}}\right)}_{+90}\left[1 - \left(\frac{f}{\hat{\omega}}\right)^2\right] \qquad \overline{v'w'} = \frac{g\hat{\omega}}{N^2}\overline{v'\left(\frac{T'}{\bar{T}}\right)}_{+90}\left[1 - \left(\frac{f}{\hat{\omega}}\right)^2\right]$$

- **Up-going (down-going)** IGWs have prevalently **northwest** and **southwest (northeast)** momentum fluxes.

Possible sources

1. For Upward propagating IGWs
- **1) Orograph**
  - ▶ **transantarctic mountains**
- **2) Spontaneous imbalanced flow**

2. For Downward propagating IGWs
- **1) Polar vortex during wintertime**
- **2) Reflection of up-going GWs**
- **3) Spontaneous imbalanced flow**

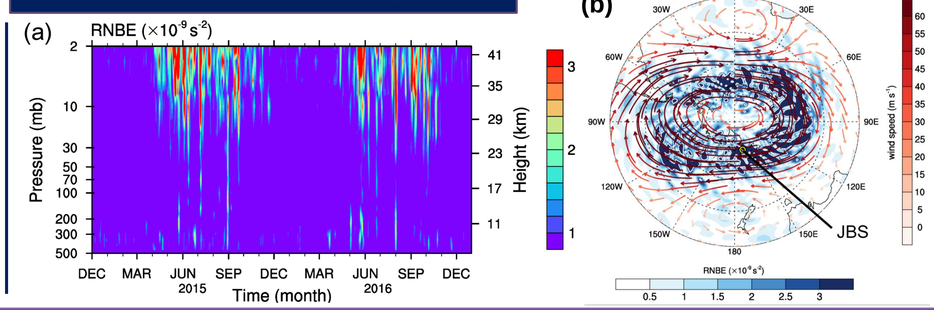

Figure 10. (a) Vertical distribution **ΔNBE** from December 2014 to December 2016 and (b) horizontal distribution of **ΔNBE** at 3 hPa for 6th September 2015 (down-going IGW is observed at JBS)

- **Higher ΔNBE** appeared from **Apr to Oct** above z = 25 km by **polar stratospheric jet.**
  - ▶ GWs could be excited by the **imbalance** processes.
- When the down-going IGWs appear, **high ΔNBE** was observed above **JBS**.

Future work

- ✓ Investigation of wave sources based on the studies of **3-D ray-tracing model of GWs and simulation**

The results are reported to the paper "Inertia-Gravity Waves Revealed in Radiosonde Data at Jang Bogo Station, Antarctica (74˚37'S, 164˚13'E). Part I: Characteristics, Energy and Momentum Flux", which is submitted to *JGR-Atmosphere* (in review).

Acknowledgments This work was supported by the Korea Polar Research Institute projects (KOPRI, PE18020)